

# A User Interface for Robot-Assisted Diagnostic Ultrasound

P. Abolmaesumi, S.E. Salcudean, W.H. Zhu, S.P. DiMaio and M.R. Sirouspour

The University of British Columbia  
Department of Electrical and Computer Engineering  
Vancouver, B.C., Canada, V6T 1Z4  
*puranga@ece.ubc.ca, tims@ece.ubc.ca*

## Abstract

*A robot-assisted system for medical diagnostic ultrasound has been developed by the authors. This paper presents key features of the user interface used in this system. While the ultrasound transducer is positioned by a robot, the operator, the robot controller, and an ultrasound image processor have shared control over its motion. Ultrasound image features that can be selected by the operator are recognized and tracked by a variety of techniques. Based on feature tracking, ultrasound image servoing in three axes has been incorporated in the interface and can be enabled to automatically compensate, through robot motions, unwanted motions in the plane of the ultrasound beam. The stability and accuracy of the system is illustrated through a 3D reconstruction of an ultrasound phantom.*

## 1 Introduction

Medical ultrasound exams often require that ultrasound technicians hold the transducers in awkward positions for prolonged periods of time, sometimes exerting large forces. A number of studies indicate that they suffer from an unusually high incidence of musculoskeletal disorders (e.g. [16]).

Motivated initially by the need to alleviate these problems and to present a more ergonomic interface to the ultrasound technicians, a teleoperation approach to diagnostic ultrasound has been proposed. The system consists of a master hand controller, a slave manipulator that carries the ultrasound probe, and a computer control system that allows the operator to remotely position the ultrasound transducer relative to the patient's body. An inherently safe, light, back-drivable, counterbalanced robot has been designed and tested for use in carotid artery examinations, the purpose of which is to diagnose occlusive disease in the left and right common carotid arteries – a major cause of strokes [14].

The motion of the robot arm is based on measured positions and forces, acquired ultrasound images, and/or taught position and force trajectories. The system uses a shared control approach that is capable of achieving motion, force and image control simultaneously.

The ability to interactively position the ultrasound probe via a teleoperated system, while being assisted with force and image controllers, has major advantages over other similar interfaces for ultrasound examination. In [10], a Mitsubishi PA-10 industrial robot was used with a force controller to assist ultrasound technicians to move the ultrasound probe against the patient's body. The ultrasound probe can only be moved by the robot, through a pre-specified trajectory, which limits the flexibility of the examination. No shared control, teleoperation or ultrasound image servoing was reported. Other approaches, such as [4, 9], focus primarily on providing an interface for 3D ultrasound image reconstruction.

In addition to the ergonomic benefits, the ability to remotely position the ultrasound probe could also be used in teleradiology [1]. Although a number of interfaces for teleultrasound examinations have been proposed in the literature [15, 5], all of them require that an ultrasound technician be present at the examination site in order to manipulate the probe under the supervision of a remote radiologist, via real-time visual and voice interaction. Our proposed system allow the radiologist to view *and to manipulate* the ultrasound transducer at the remote site.

The ability to automatically guide the ultrasound probe as a function of its acquired images, an approach termed “ultrasound image servoing”, could be a useful feature for diagnostic examinations when used in conjunction with human supervisory control, in order to reduce operator fatigue [2]. During the ultrasound examination, the operator interacts with a graphical user interface and a hand controller. The resulting op-

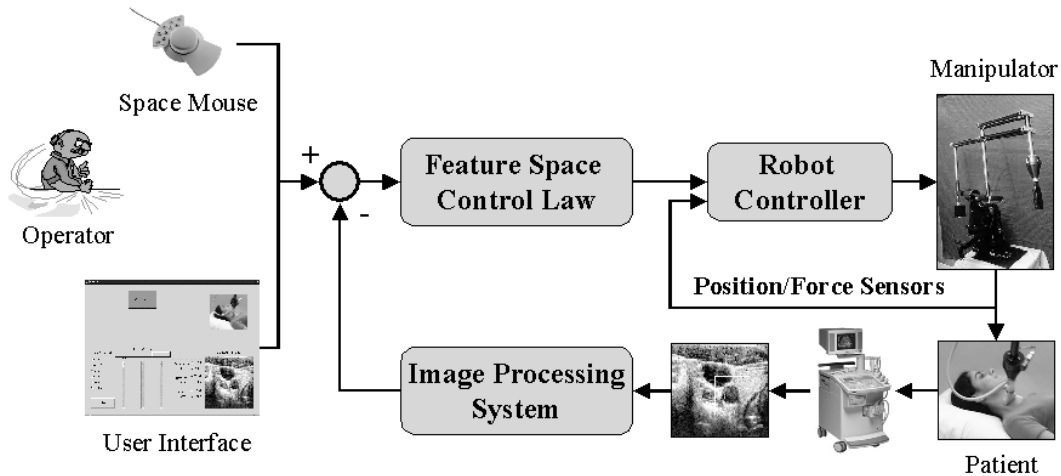


Figure 1: Block diagram of the ultrasound robot system.

erator commands are coordinated with a local visual servoing system in order to control the robot, and thus the ultrasound-probe motion.

Image servoing in the control of three degrees of freedom of the robot is being addressed in this paper. Section 2 describes the system setup. Section 3 presents the theory behind ultrasound image servoing, along with the experimental results. An application of the system to reconstruct an ultrasound phantom in 3D is described in Section 4. Finally, Section 5 provides a summary and concluding remarks.

## 2 System Setup

Figure 1 shows the block-diagram of the experimental setup. The system consists of a user interface, a slave manipulator carrying the ultrasound probe, and a computer control system.

### 2.1 The User Interface

The operator interacts with the system through the user interface, which consists of a master hand controller (a SpaceMouse/Logitech Magellan [6]) and a graphical user interface (GUI). The GUI was written using the `gtk+` library under the Linux operating system. Figure 2 shows a screen shot of the GUI. It allows the operator to activate/deactivate the robot, to enable/disable the force control and the visual servoing and to enable/disable different degrees of freedom of the robot. Other features such as changing the sensitivity of the robot to the user positioning commands and switching the robot working frame from the world to the probe and vice versa are also incorporated in the GUI.

Ultrasound images are captured in real-time and are displayed in the GUI. A 3D rendered model of the ultrasound probe, which displays the orientation of the transducer in real-time, is incorporated within the GUI. One or more features can be selected from the ultrasound image by using the mouse pointer. These features are passed to the image controller to compensate for motions in the plane of the ultrasound beam, the goal of which is to maintain features at the desired position in the image.

The velocity of all axes of the robot can be controlled by the Magellan mouse. All buttons and sliders in the GUI can be controlled by the keypad of the Magellan mouse.

### 2.2 Ultrasound Robot

A lightweight robot with limited force capability has been designed for teleoperated ultrasound examinations [12]. The robot moves fast enough to allow ultrasound examination to take place at a pace close to that achieved by the unassisted sonographer. In addition, the robot joints are backdrivable so that the arm can be pushed out of the way if necessary and controlled effectively in force mode. During the ultrasound examination, the ultrasound transducer is carried by the end-effector of the robot. Small motor driving torques are required to generate a maximum force of 10 N at the end-effector, due to the fully counterbalanced mechanical design. This results in a system that is safe in the case of a power failure. A resolution of 0.1mm for translation and  $0.09^\circ$  for rotation of the end-effector has been achieved.



Figure 2: Graphical user interface.

### 2.3 Robot Controller

The control approach is explained in [17]. Its objective is to let a linear combination of the velocity and scaled force of the ultrasound probe track the hand controller command (displacement). There is no explicit switching between the contact and free motion states. Safety is insured by including a control “command reset” or “disturbance accommodation” function that never allows position errors to be large. The controller uses the measured probe positions and forces, the acquired ultrasound images, and/or the commanded position and force trajectories simultaneously in a shared control approach to control the robot arm. The controller runs on a VxWorks<sup>TM</sup> real-time operating system.

### 3 Ultrasound Image Servoing

One of the main features of the current system is its ability to visually track features in ultrasound images in real-time. This could help ultrasound technicians in guiding the motion of the ultrasound probe during the examination. The image processing system captures the ultrasound images at a rate of 30 frames/s by using a MV-delta frame grabber. The Star-Kalman motion tracking algorithm [2, 3] provides the image controller with the required feature coordinates (e.g. the center of the carotid artery) to control the robot. The feasibility of the ultrasound image servoing to control three axes of the robot can be determined by examining the

ultrasound image Jacobian, which relates differential changes in the image features to differential changes in the configuration of the robot. Figure 3 illustrates the concept. Let  $P_i = [u_i, v_i]^T$  be a feature point in the plane of the ultrasound image with coordinates  $[e^x, e^y, e^z]^T$  in the probe-attached frame. Assuming an orthographic projection model [8] with scale  $a$  for the ultrasound image and that  $P_i$  remains in the image plane, the coordinates of  $P_i$  in the two-dimensional ultrasound image become  $[u_i - u_0, 0, v_i]^T = [a^e x, 0, a^e z]^T$ , where  $[u_0, v_0]^T$  is the center of the ultrasound image. It can be shown that

$$\begin{bmatrix} \dot{u}_i \\ \dot{v}_i \end{bmatrix} = \begin{bmatrix} a & 0 & 0 & 0 & -v_i & 0 \\ 0 & 0 & a & 0 & u_i - u_0 & 0 \end{bmatrix} e^{\dot{X}} = J_{v_i} e^{\dot{X}} \quad (1)$$

where  $e^{\dot{X}}$  are the translational and angular end-effector velocities in end-effector coordinates and  $J_{v_i} \in \mathfrak{R}^{2n \times 6}$  is the ultrasound image Jacobian matrix. If several points are considered in the image, similar pairs of rows will be added to (1). The rank of the resulting Jacobian is at most three. Two or more feature points with motions not along the lines connecting them to each other will generate a Jacobian of rank three. Thus, as expected, with non-trivial ultrasound images, it is possible to control the motion of the ultrasound transducer in its image plane in three degrees of freedom. The visual controller, depicted in Figure 4, is described by:

$$e^{\dot{X}} = -J_{v_i}^\dagger [K_d (f_i - f_r) - \dot{f}_r], \quad (2)$$

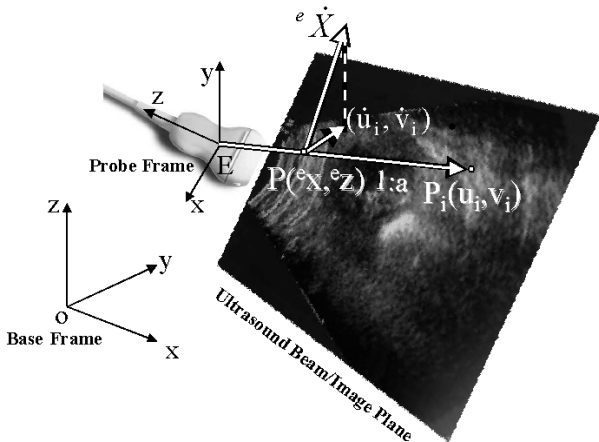


Figure 3: Definition of the frames for the ultrasound robot.

where  $f_i = [u_i, v_i]^T$  is the actual image feature location in the ultrasound image,  $f_r$  is its desired location,  $K_d$  is the controller gain and  $J_{v_i}^\dagger$  is the pseudo-inverse of  $J_{v_i}$ . Replacing  $J_{v_i}$  from (1) in (2) and assuming that the dynamics of the robot control loop are negligible relative to the image control loop, the following equation is derived:

$$\dot{f}_i + K_d f_i = K_d f_r + \dot{f}_r, \quad (3)$$

which guarantees that image feature servoing

$$(f_i) \longrightarrow (f_r) \quad (4)$$

can be achieved.

An ultrasound phantom has been designed to validate the visual servoing algorithm. Figure 5 illustrates a CAD model of the phantom. Three plastic tubes are positioned in a solution [11] along three different axes in the phantom. Ultrasound image servoing at rates as high as 30 Hz has been achieved to control up to three axes of the robot, while tracking one or two features in the ultrasound image in real-time. With the probe coordinate frame illustrated in Figure 3, the control axes are the translations along the  $x$ -axis and  $z$ -axis, while the rotation is about the  $y$ -axis. Figure 6 shows the ultrasound image servoing performance for one of the axes. For this experiment, a feature (center of one of the pipes in the phantom ultrasound image) is selected before enabling the visual servoing. While the operator is moving the probe along the  $y$  axis, the feature position is maintained in the center of the image automatically.

The performance of the system while tracking two features (center of two pipes in the phantom ultrasound image) simultaneously is shown in Figure 7.

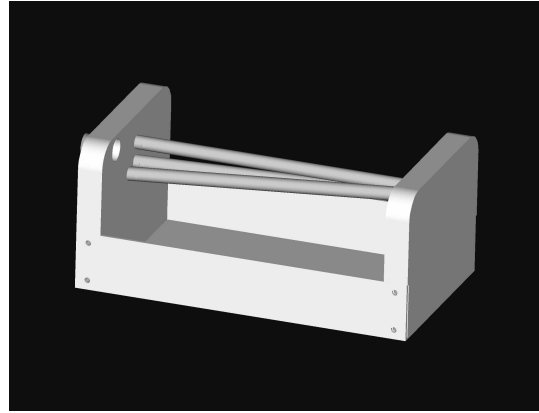


Figure 5: A CAD model of the ultrasound phantom.

The two features are moved away from their reference points at  $t = .7s$  by moving the robot along the  $x$ -axis and are moved back by the image servoing action. In this experiment,  $K_d = I_{4 \times 4}$  Hz.

## 4 3D Ultrasound Imaging

The current system can be used for other applications such as 3D ultrasound imaging. Since the location of the ultrasound transducer can be determined via the forward kinematics of the slave manipulator, three-dimensional ultrasound images can be reconstructed from a series of two-dimensional image slices. The robot is used to reconstruct a 3D model of the tubes in the phantom. The ultrasound image servoing has been used to center the pipes in the image during the ultrasound examination. Two different 3D reconstruction methods have been implemented as discussed in the subsections that follow.

### 4.1 Stradx

Stradx [7] is a tool for the acquisition and visualization of 3D ultrasound images using a conventional 2D ultrasound machine and an Ascension Bird<sup>TM</sup> position sensor. The contours that specify an anatomic region of interest are drawn in a series of two-dimensional image slices by the operator. These contours are mapped to a 3D space by using the position information provided by the sensor. In this application, the measured robot/probe position was substituted in place of the sensor data as input to the Stradx program. Since the resolution of the robot is higher than that of the Bird sensor and since it is independent of metal in the surrounding environment, the system provides a powerful tool for accurate 3D reconstruction of ultrasound images. Figure 8 shows the 3D reconstruction of the ultrasound phantom using this approach.

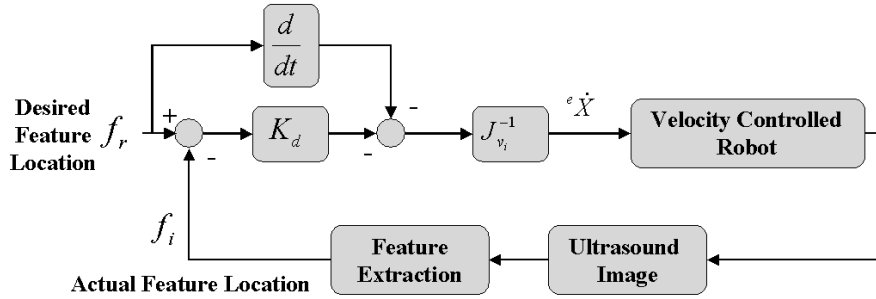


Figure 4: Ultrasound image controller.

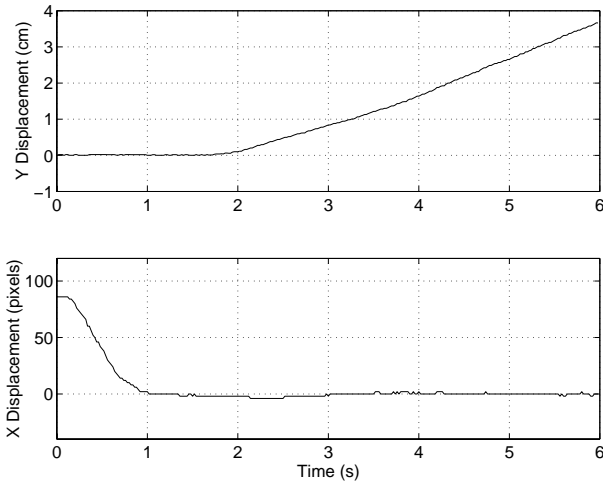


Figure 6: Experimental results for image servoing in single axis.

## 4.2 Star-Kalman Based Reconstruction

By using the Star-Kalman algorithm [2] to extract each pipe's contour in the ultrasound image in real-time and the inverse kinematics of the robot to map each contour to the world coordinates, a 3D image of each pipe is reconstructed. Figure 9 shows a partially reconstructed image. No smoothing filter has been used.

In contrast to the Stradx reconstruction approach, where the operator has to specify the contour of the desired region in each ultrasound image frame separately, this method extracts each pipe's contour automatically in real-time. In addition, the data storage requirements are much lower than that of the Stradx approach, as only the contour coordinates are necessary for 3D reconstruction. However, the image is substantially noisier.

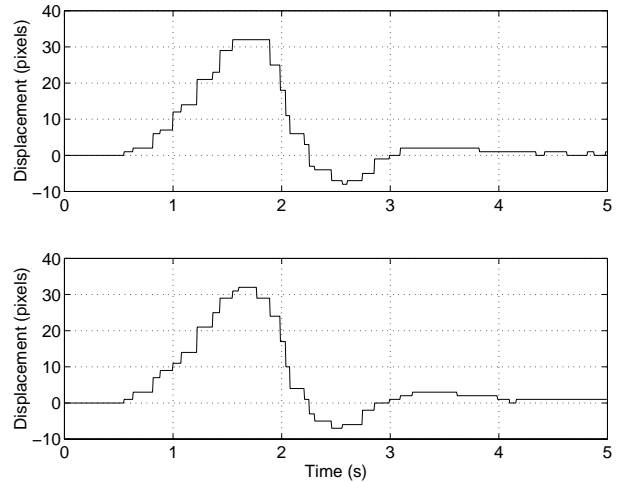


Figure 7: Experimental results for image servoing in three axes; the position of the two features are changed by moving the robot in  $x$  direction.

## 5 Summary and Conclusions

A new medical ultrasound examination system that uses a robot to remotely position the ultrasound probe is presented. The system uses a shared control approach that is capable of achieving motion, force and image control simultaneously. An ultrasound image servoing capability is embedded in the system. Ultrasound visual servoing to control three axes of the robot has been demonstrated. An application of the system in 3D ultrasound image reconstruction has also been described.

In the future, the passive mouse will be replaced by a PowerMouse haptic interface [13], in order to realize bilateral teleoperation with force feedback. Also, the system will be used and tested for ultrasound diagnostic at the Vancouver General Hospital, UBC. A human factors study to compare the presented approach with that of the conventional ultrasound examination is also

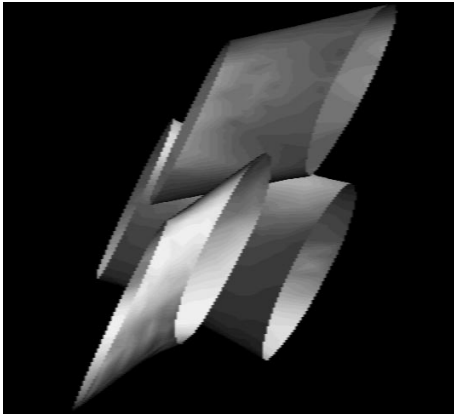


Figure 8: Partial 3D image reconstruction of the ultrasound phantom.

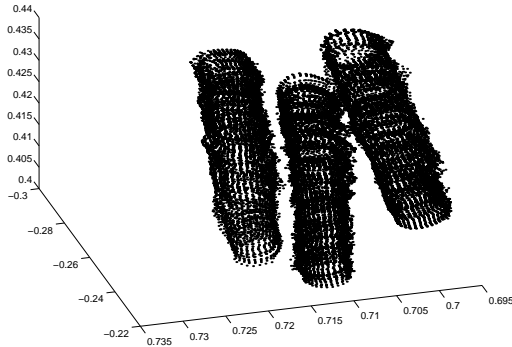


Figure 9: Partial 3D image reconstruction of the ultrasound phantom by using the Star-Kalman contour extraction method.

under way.

## References

- [1] P. Abolmaesumi, S.P. DiMaio, S.E. Salcudean, R. Six, W.H. Zhu, and L. Filipozzi. Teleoperated robot-assisted diagnostic ultrasound. Demo Presentation, IRIS/PREARN 2000, Montreal.
- [2] P. Abolmaesumi, S.E. Salcudean, and W.H. Zhu. Visual servoing for robot-assisted diagnostic ultrasound. *World Congress on Medical Physics and Biomedical Engineering*, Chicago, 2000.
- [3] P. Abolmaesumi, M.R. Sirouspour, and S.E. Salcudean. Real-time extraction of carotid artery contours from ultrasound images. *Computer-Based Medical Systems*, pages 181–186, Texas, June 2000.
- [4] K. Baba, K. Satch, S. Satamoto, T. Okai, and I. Shiego. Development of an ultrasonic system for three-dimensional reconstruction of the foetus. *J. Perinat. Med.*, 17, 1989.
- [5] W.J. Chimiak, R.O. Rainer, N.T. Wolfman, and W. Covitz. Architecture for a high-performance tele-ultrasound system. *Medical Imaging: PACS Design and Evaluation: Engineering and Clinical Issues*, 2711:459–465, Newport Beach, CA, 1996.
- [6] J. Dietrich, G. Plank, and H. Kraus. Optoelectronic system housed in plastic sphere. Europ. Patent No. 0 240 023; US-Patent No. 4,785,180; JP-Patent No. 1 763 620.
- [7] A.H. Gee and R.W. Prager. Sequential 3d diagnostic ultrasound using the stradx system. *MICCAI'99*, Cambridge, UK, September 1999.
- [8] S. Hutchinson, G. Hager, and P.I. Corke. A tutorial on visual servo control. *IEEE Trans. on Rob. Auto.*, 12(5):651–670, October 1996.
- [9] R. Ohbuchi, D. Chen, and H. Fuchs. Incremental volume reconstruction and rendering for 3-d ultrasound imagine. *Vis. Biomed. Comput.*, pages 312–323, 1992.
- [10] F. Pierrot, E. Domre, and E. Dgoulange. Hippocrate: A safe robot arm for medical applications with force feedback. *Medical Image Analysis*, 3:285–300, 1999.
- [11] D.W. Rickey, P.A. Picot, D.A. Christopher, and A. Fenster. A wall-less vessel phantom for doppler ultrasound studies. *Ultrasound in Medicine and Biology*, 21(9):1163–76, 1995.
- [12] S.E. Salcudean, G. Bell, S. Bachmann, W.H. Zhu, P. Abolmaesumi, and P.D. Lawrence. Robot-assisted diagnostic ultrasound - design and feasibility experiments. *MICCAI'99*, Cambridge, UK, September 1999.
- [13] S.E. Salcudean and N.R. Parker. 6-dof desk-top voice-coil joystick. *6<sup>th</sup> Symp. Haptic Inter. for Virtual Env. and Teleop. Sys., Intl. Mech. Eng. Congr. Exp., (ASME Winter Annual Meeting)*, 61:131–138, November 16-21 Dallas, Texas, 1997.
- [14] S.E. Salcudean, W.H. Zhu, P. Abolmaesumi, S. Bachmann, and P.D. Lawrence. A robot system for medical ultrasound. *ISRR'99*, pages 152–159, Oct. 9–12 Snowbird, Utah, 1999.
- [15] J. Sublett, B. Dempsey, and A.C. Weaver. Design and implementation of a digital teleultrasound system for real-time remote diagnosis. *Computer-Based Medical Systems*, pages 292–299, June Texas, 1995.
- [16] H.E. Vanderpool, E.A. Friis, B.S. Smith, and K.L. Harms. Prevalence of carpal tunnel syndrome and other work-related musculoskeletal problems in cardiac sonographers. *Journal of Occupational Medicine*, 35:604–610, June 1993.
- [17] W.H. Zhu, S.E. Salcudean, S. Bachman, and P. Abolmaesumi. Motion/force/image control of a diagnostic ultrasound robot. *Proc. IEEE Int. Conf. Rob. Auto.*, San Francisco, 2000.